TFAP2C is a key regulator of intrauterine trophoblast cell invasion and deep hemochorial placentation

Esteban M. Dominguez[1,*], Ayelen Moreno-Irusta[1], Regan L. Scott[1], Khursheed Iqbal[1,†], and Michael J. Soares[1,2,3,*]

[1]Institute for Reproductive and Developmental Sciences, Department of Pathology & Laboratory Medicine, University of Kansas Medical Center, Kansas City, Kansas 66160, [2]Department of Obstetrics and Gynecology, University of Kansas Medical Center, Kansas City, Kansas 66160, [3]Center for Perinatal Research, Children's Mercy Research Institute, Children's Mercy, Kansas City, MO 64108

[†]Present address: Department of Animal and Food Sciences, Oklahoma State University, Stillwater, Oklahoma

***Correspondence: edominguez@kumc.edu or msoares@kumc.edu**

Conflict of interests

The authors have declared that no conflict of interest exists.

Abstract

The transcription factor AP-2 gamma (**TFAP2C**) has been identified as a key regulator of the trophoblast cell lineage and hemochorial placentation. The rat possesses deep placentation characterized by extensive intrauterine trophoblast cell invasion, which resembles human placentation. Initially, we examined *Tfap2c* expression in the rat placentation site and demonstrated its presence in multiple trophoblast cell lineages, including invasive trophoblast cells situated within the uterine-placental interface. Global genome-editing was used to explore the biology of *Tfap2c* in rat placentation. Homozygous global disruption of *Tfap2c* resulted in prenatal lethality between gestation days 8.5 and 9.5. Although, global disruption of one *Tfap2c* allele was compatible with survival, this heterozygous condition was surprisingly associated with diminished invasive trophoblast cell infiltration into the uterus. Since *Tfap2c* is expressed in multiple trophoblast cell lineages, we next explored the role of TFAP2C in the invasive trophoblast cell lineage using Cre-lox conditional mutagenesis. Invasive trophoblast cell-specific disruption of *Tfap2c* resulted in inhibition of intrauterine trophoblast cell invasion and intrauterine and postnatal growth restriction. In contrast to the global disruption of *Tfap2c*, the invasive trophoblast cell lineage was not impaired following conditional monoallelic disruption of *Tfap2c*. In summary, TFAP2C contributes to the progression of distinct stages of placental development. TFAP2C is a driver of early events in trophoblast cell development and reappears later in gestation as an essential regulator of the invasive trophoblast cell lineage. A subset of TFAP2C actions on trophoblast cells are dependent on gene dosage.

Introduction

The placenta is a transient organ that ensures viviparity and optimal fetal development (1–3). The human and rat possess a hemochorial placenta (4, 5), which is composed of specialized cellular constituents termed trophoblast cells (6). Among the trophoblast cell lineages contributing to the placentation site are invasive trophoblast cells, which in the human are referred to as extravillous trophoblast cells (7). Human and rat placentation sites are characterized by deep intrauterine trophoblast cell invasion (8–10). Invasive trophoblast cells facilitate the erosion of maternal uterine spiral arteries permitting a direct flow of maternal nutrients to trophoblast cells (8, 11–15). Uterine vasculature remodeling is a critical process ensuring a successful pregnancy outcome (13, 16, 17). There is a paucity of knowledge regarding regulatory mechanisms controlling development of the invasive trophoblast cell lineage and trophoblast cell-guided uterine spiral remodeling.

Members of the transcription factor AP-2 (**TFAP2**) family are key regulators of embryonic and extraembryonic development (18, 19). TFAP2C distinguishes itself as a regulator of the trophoblast cell lineage and hemochorial placentation (20–22). In the mouse, global disruption of the *Tfap2c* locus results in abnormalities within the trophoblast cell lineage and prenatal lethality prior to placentation (23, 24). Although, TFAP2C is an established regulator of the earliest stages of trophoblast cell lineage development (25–28), placental expression profiles and target gene occupancy also implicate TFAP2C in the regulation of multiple processes impacting mammalian placentation and placental function (29–40). Included in this broad spectrum of TFAP2C

actions on placentation is its potential involvement in invasive trophoblast cell biology (38–41).

In this report, we present the results of in vivo experimentation directed toward elucidating the physiological role of TFAP2C in the developing hemochorial placenta with a focus on trophoblast cell-guided events within the uterine-placental interface. We show that TFAP2C possesses essential roles during distinct stages of placental development. TFAP2C is an essential regulator of early placental morphogenetic events and reappears in a critical capacity for invasive trophoblast cell lineage development. Finally, elements of TFAP2C actions on placentation are dose dependent.

Results

TFAP2C expression within the placentation site

The rat hemochorial placenta is comprised of multiple lineages of trophoblast cells arranged into distinct compartments, including the labyrinth zone, junctional zone, and uterine-placental interface (42, 43) (Figure 1). The labyrinth zone is the site of maternal-fetal nutrient/waste transfer (44), whereas the junctional zone is composed of endocrine cells targeting the maternal environment and the site where invasive trophoblast cells arise (42, 43, 45). Cell composition of the uterine-placental interface is dynamic, including an increase in the infiltration of invasive trophoblast cells as gestation proceeds (9, 38). Intrauterine invasive trophoblast cells invade into the stroma located between uterine blood vessels (interstitial) and within uterine blood vessels (endovascular). *Tfap2c* transcripts were detected within the uterine-placental interface and increased during pregnancy (Supplemental Figure 1A). In situ hybridization was used to determine the distribution of *Tfap2c* transcripts within the hemochorial placenta. At gestation day (**gd**)

85 9.5, *Tfap2c* was prominently expressed in the ectoplacental cone (Figure 1A). *Tfap2c*
86 transcripts were also localized to the anti-mesometrial uterine deciduum (Figure 1A). As
87 gestation advanced (gd 11.5), *Tfap2c* expression was observed within trophoblast cells of
88 the developing placenta (Figure 1B). On gd 18.5, *Tfap2c* was abundantly expressed within
89 the junctional zone and in invasive trophoblast cells of the uterine-placental interface
90 (Figure 1C-E). The presence of *Tfap2c* transcripts in the trophoblast cell lineage was
91 supported by its colocalization with keratin 8 (***Krt8***), a pan-trophoblast cell marker (Figure
92 1A-C). Expression of *Tfap2c* transcripts in invasive trophoblast cells was further
93 demonstrated by co-localization with prolactin family 7, subfamily b, member 1 (*Prl7b1*)
94 transcripts (Figure 1D and E), an invasive trophoblast cell-specific transcript, and is
95 consistent with single cell RNA-sequencing of the of the uterine-placental interface
96 (Supplemental Figure 1B) (38). TFAP2C protein was distributed in invasive trophoblast
97 cells of the uterine-placental interface and throughout the junctional zone, replicating the
98 distribution of *Tfap2c* transcripts at gd 18.5 (Supplemental Figure 2). Within the invasive
99 trophoblast cell lineage, TFAP2C transcript and protein were localized to both
100 endovascular and interstitial trophoblast cells (Figure 1E**,** Supplemental Figure 3). *Tfap2c*
101 transcripts were localized to most trophoblast cell populations within the junctional zone,
102 including a smaller subset of invasive trophoblast progenitor cell populations (*Prl7b1*
103 positive; **Figure 1F**).
104
105 **Global deletion of *Tfap2c* leads to prenatal lethality**
106 Next, we investigated the in vivo role of *Tfap2c* in rat placenta development using
107 CRISPR/Cas9 genome editing. DNA-binding and dimerization domains encoded by Exon
108 4 of the *Tfap2c* gene were targeted (Supplemental Figure 4A). A germ line mutant rat was
109 generated possessing a 308-bp deletion within Exon 4 (Supplemental Figure 4B). The

110 deletion resulted in a frameshift and a premature stop codon (Supplemental Figure 4C).
111 Polymerase chain reaction (**PCR**) products corresponding to wild type and mutant alleles
112 were identified by genotyping (828 bp versus 520 bp, respectively, Supplemental Figure
113 4D). Null *Tfap2c* conceptuses (-/-) were obtained by mating heterozygous (+/-) *Tfap2c*
114 females and males. Breeding results collected throughout pregnancy and postnatally,
115 including Mendelian ratios, are presented in Supplemental Table 1. Null *Tfap2c*
116 conceptuses were viable until gd 8.5, which temporally coincides with the onset of
117 placental morphogenesis. This observation agrees with the timing of embryonic demise
118 observed following global *Tfap2c* mouse gene disruption (23, 24). Interestingly, we
119 observed an unexpected reduction in the number of surviving heterozygous pups
120 generated from *Tfap2c*$^{+/-}$ x *Tfap2c*$^{+/-}$, which prompted an investigation of placental
121 development in conceptuses possessing a single *Tfap2c* mutant allele.
122

123 **Decreased *Tfap2c* gene dosage leads to a failure in intrauterine trophoblast cell**
124 **invasion**

125 To explore possible *Tfap2c* gene dosage effects, *Tfap2c*$^{+/+}$ females and *Tfap2c*$^{+/-}$ males
126 were mated, and pregnancies assessed at gd 18.5. *Tfap2c*$^{+/+}$ and *Tfap2c*$^{+/-}$ placentation
127 sites exhibited a similar organizational structure, including a labyrinth zone, junctional
128 zone, and a uterine-placental interface (Figure 2A). We next assessed infiltration of
129 invasive trophoblast cells into the uterine-placental interfaces of *Tfap2c*$^{+/+}$ versus *Tfap2c*$^{+/-}$
130 placentation sites by monitoring the distribution of cytokeratin protein expression (9, 38)
131 (Figure 2B) and *Prl7b1* mRNA (46) (Figure 2C), both representing indices of invasive
132 trophoblast cells. The uterine-placental interface of *Tfap2c*$^{+/-}$ placentation sites were
133 depleted of invasive trophoblast cells (Figure 2B and C). Both interstitial and endovascular
134 invasive trophoblast cells were diminished in the uterine-placental interface of *Tfap2c*$^{+/-}$

135 placentation sites. This result was supported by quantification of the depth of invasion of
136 cytokeratin positive cells into the uterine parenchyma (Figure 2D). The depletion of
137 invasive trophoblast cells in the uterine-placental interface of *Tfap2c*$^{+/-}$ placentation sites
138 was further supported by diminished expression of several invasive trophoblast cell
139 associated transcripts (*Krt7, Krt8, Krt18, Prl7b1, Prl5a1, Cdkn1c, Cited2, Plac1, Peg3,*
140 *Tfpi;* (38) (Figure 2E). Similar findings were recorded when placentation sites were
141 interrogated from pregnancies generated from *Tfap2c*$^{+/-}$ females mated to *Tfap2c*$^{+/+}$ males
142 (Supplemental Figure 5 A-D).
143 However, breeding combinations did differentially affect postnatal heterozygote
144 offspring viability and heterozygote fetal and placental weights. Postnatal heterozygote
145 viability was prominently decreased in female *Tfap2c*$^{+/-}$ x male *Tfap2c*$^{+/-}$ but not in female
146 *Tfap2c*$^{+/+}$ x male *Tfap2c*$^{+/-}$ or female *Tfap2c*$^{+/-}$ x male *Tfap2c*$^{+/+}$ breeding combinations
147 (Supplemental Table 1-3). Genotypic differences in fetal, placenta, junctional zone, and
148 labyrinth zone weights at gd 18.5 were observed among breeding combinations. Mating
149 *Tfap2c*$^{+/+}$ females with *Tfap2c*$^{+/-}$ males was associated with significant decreases in
150 heterozygote placenta, junctional zone, and labyrinth zone weights (Figure 2F), whereas
151 only heterozygote fetal weights were significantly decreased by mating *Tfap2c*$^{+/-}$ females
152 with *Tfap2c*$^{+/+}$ males (Supplemental Figure 5 E). Some of these differences might be
153 associated with *Tfap2c* gene dosage effects on the maternal environment.
154

155 **Invasive trophoblast cell conditional *Tfap2c* mutagenesis**

156 The impact of TFAP2C dosage on invasive trophoblast cell development prompted a
157 direct analysis of the importance of TFAP2C on the invasive trophoblast cell lineage. We
158 generated an invasive trophoblast cell-specific *Tfap2c* gene disruption using Cre/loxP
159 system. CRISPR/Cas9 genome editing was used to insert loxP sites flanking Exon 4 of

160 the *Tfap2c* gene (Figure 3A). *Tfap2c* floxed (***Tfap2c***$^{f/f}$) rats were mated with *Prl7b1-Cre*
161 rats (47). Cre recombinase is specifically targeted to invasive trophoblast cells in *Prl7b1-*
162 *Cre* rats (47). TFAP2C protein was present in lysates of the *Tfap2c*$^{f/f}$ uterine-placental
163 interface but not in lysates of the *Tfap2c*$^{d/d}$ uterine-placental interface (Figure 3B).
164 Immunostaining supported depletion of TFAP2C from the gd 18.5 uterine-placental
165 interface but not from the JZ of *Tfap2c*$^{d/d}$ placentation sites (Figure 3C). Our ability to
166 modulate TFAP2C in the invasive trophoblast cell lineage led us to evaluate a potential
167 role for TFAP2C in regulating the invasive trophoblast cell lineage.
168
169 **TFAP2C-dependent intrauterine trophoblast cell invasion**
170 Intrauterine trophoblast cell invasion was assessed in *Tfap2c*$^{f/f}$ and *Tfap2c*$^{d/d}$
171 placentation sites. At gd 18.5 invasive trophoblast cells were present throughout the
172 *Tfap2c*$^{f/f}$ uterine-placental interface but were not detected in the *Tfap2*$^{d/d}$ uterine-placental
173 interface (Figure 4 A-C). Interstitial and endovascular invasive trophoblast cells were
174 absent from the uterine-placental interface of *Tfap2c*$^{d/d}$ placentation sites. The depletion
175 of invasive trophoblast cells in the uterine-placental interface of *Tfap2c*$^{d/d}$ placentation
176 sites was further supported by diminished expression of several invasive trophoblast cell-
177 associated transcripts (*Krt7, Krt8, Krt18, Prl7b1, Prl5a1, Cdkn1c, Cited2, Plac1, Peg3,*
178 *Tfpi*; Figure 4D). In contrast to the global disruption of *Tfap2c*, migration of invasive
179 trophoblast cells into the uterus was not impaired following conditional monoallelic
180 disruption of *Tfap2c* (Supplemental Figure 6). Single cell RNA-sequencing and single
181 nucleus assay for transposase-accessible chromatin-sequencing datasets (38, 41) reveal
182 a network of genes potentially regulated by TFAP2C in rat invasive trophoblast cells that,
183 include candidate contributors to remodeling extracellular matrix, cytoskeleton
184 restructuring, regulation of cell movement, and transcriptional regulators that target genes

185 encoding other proteins affecting the invasive trophoblast phenotype (Figure 4E;
186 Supplemental Dataset 1). Thus, TFAP2C has a fundamental role in regulating the invasive
187 trophoblast cell lineage, especially movement of invasive trophoblast cells into the uterus,
188 and a list of downstream effectors are available to investigate mechanisms underlying
189 TFAP2C actions.
190

191 **Invasive trophoblast cells and natural killer (NK) cells exhibit a reciprocal**
192 **distribution within the uterine-placental interface**

193 At midgestation, NK cells are an abundant constituent of the uterine-placental interface
194 (48). As gestation progresses, NK cells become depleted as trophoblast cells invade the
195 uterine-placental interface (48). Interestingly, we observed a retention of NK cells in
196 *Tfap2c*$^{d/d}$ uterine-placental interfaces depleted of invasive trophoblast cells (Figure 5A).
197 This observation was further supported by increased expression of NK cell-associated
198 transcripts (*Prf1, Klrb1c, Klrb1a, Klrb1, Ncr1*; Figure 5B) within *Tfap2c*$^{d/d}$ uterine-placental
199 interfaces. These findings reinforce the observation that fundamental changes occur in
200 the *Tfap2c*$^{d/d}$ uterine-placental interface and imply that invasive trophoblast cells affect
201 cellular dynamics within the uterine-placental interface.
202

203 **Invasive trophoblast cells impact prenatal and postnatal growth**

204 We next investigated whether the presence of invasive trophoblast cells within the
205 uterine-placental interface affected prenatal or postnatal growth. Depletion of invasive
206 trophoblast cells as observed in *Tfap2c*$^{d/d}$ placentation sites was associated with
207 intrauterine placental growth restriction, including both junctional zone and labyrinth zone
208 compartments, and fetal growth restriction at gd 18.5 (Figure 6A). The adverse effects of
209 invasive trophoblast cell depletion on fetal weight extended to postnatal offspring growth.

210 Depletion of invasive trophoblast cells was associated with decreased postnatal body
211 weight (Figure 6B). The results are consistent with invasive trophoblast cells supporting
212 the nutrient demands required for optimal intrauterine growth. Deficits acquired prenatally
213 were sustained during the first three weeks of postnatal life.
214
215 **Discussion**
216 Placentation is a critical adaptation ensuring the success of viviparity (5, 49). Gene
217 manipulated animal models and trophoblast stem cells have provided insights into gene
218 regulatory networks controlling trophoblast cell lineage development and placentation
219 (21). TFAP2C figures prominently in these networks and represents a conserved
220 regulator of placentation (20–22). In the research reported here, we utilized genome-
221 edited rat models to elucidate roles for TFAP2C in placentation. The rat, like the human,
222 is a species exhibiting deep intrauterine trophoblast cell invasion (8–10). TFAP2C is
223 expressed in multiple trophoblast cell lineages of the developing rat placenta, including
224 invasive trophoblast cells residing in the uterine-placental interface. Consistent with
225 earlier reports in the mouse (23, 24), global disruption of *Tfap2c* in the rat led to prenatal
226 lethality (gd 8.5 to 9.5), prior to the initiation of placenta morphogenesis. Interestingly,
227 decreased gene dosage of *Tfap2c* (heterozygous) was compatible with pregnancy but
228 affected placentation, including diminished infiltration of invasive trophoblast cells into
229 the uterine-placental interface. A role for TFAP2C in the regulation of intrauterine
230 trophoblast cell invasion was further supported using cell lineage specific mutagenesis.
231 *Tfap2c* was conditionally disrupted in the invasive trophoblast cell lineage, which led to a
232 uterine-placental interface devoid of invasive trophoblast cells. Impairment of intrauterine
233 trophoblast cell invasion had consequences, including intrauterine and postnatal growth
234 restriction.

235

236 Involvement of TFAP2C in early events dictating trophoblast cell lineage development
237 were reinforced from phenotyping conceptuses possessing a global disruption of the
238 *Tfap2c* locus. TFAP2C is critical to activation of the trophectoderm transcriptome (36,
239 50) and development of trophectoderm (25, 26, 51, 52). Trophectoderm represents the
240 earliest stage of trophoblast cell lineage development (53, 54). The importance of
241 TFAP2C in early trophoblast cell lineage development is further exemplified by its
242 utilization in the direct reprogramming of fibroblasts to the trophoblast cell lineage (27,
243 28).

244

245 TFAP2C actions in the rat placentation site were affected by gene dosage. Monoallelic
246 disruption of *Tfap2c* resulted in the development of a rat uterine-placental interface
247 possessing a diminished number of invasive trophoblast cells. Observing a phenotype in
248 *Tfap2c* global heterozygotes was intriguing but not entirely new for *Tfap2c*.
249 Haploinsufficiency of *Tfap2c* is linked to an increased incidence of peripartum lethality
250 (55). Surviving *Tfap2c* heterozygotes exhibit postnatal growth restriction (24),
251 development of germ cell tumors (56), and hippocampal dysfunction (57). Placentation is
252 also affected by *Tfap2c* haploinsufficiency (55). The labyrinth zone compartment of the
253 mouse placenta is disorganized in *Tfp2c* heterozygotes (55). Interestingly, the invasive
254 trophoblast cell phenotype observed in global heterozygotes reported here was not a
255 feature of conceptuses with a monoallelic disruption of *Tfap2c* restricted to the invasive
256 trophoblast cell lineage. An explanation for this difference is likely connected to the wide-
257 spread involvement of TFAP2C in multiple stages of trophoblast cell differentiation (58).
258 This is supported by TFAP2C expression extending to many more trophoblast cells in
259 the junctional zone than express *Prl7b1*, the gene driving Cre recombinase expression in

our conditional mutagenesis rat model. Global *Tfap2c* haploinsufficiency at a key stage of trophoblast cell lineage development distinct from *Prl7b1*-expressing trophoblast cells must be relevant and responsive to *Tfap2c* gene dosage. Thus, *Tfap2c* gene dosage is utilized in a differentiation stage specific manner to guide trophoblast cell development.

TFAP2C is utilized at different stages of trophoblast cell development. TFAP2C is critical to the derivation of the trophoblast cell lineage and then repurposed for later stages of placentation (58), including the regulation of invasive trophoblast cell development. TFAP2C does not act alone. Context is critical for the actions of TFAP2C. The presence of other transcription factor partners and stoichiometry influence TFAP2C function during trophoblast cell development (21, 59). A short list of potential TFAP2C partners in invasive trophoblast cell development is available (38, 41).

Lastly, we have taken transcript and open chromatin profiles (38, 41) and created a path for elucidating gene involvement in the regulation of invasive trophoblast cell lineage development and its impact on the uterine-placental interface. We provide compelling evidence that TFAP2C is critical in establishing the invasive trophoblast cell lineage. Furthermore, we effectively demonstrate that the presence of invasive trophoblast cells in the uterus has consequences. Deficits in invasive trophoblast cell guided uterine transformation resulted in intrauterine and postnatal growth restriction. Most importantly, tools are in place to establish a gene regulatory network controlling development and function of the invasive trophoblast cell lineage.

In summary, TFAP2C contributes to the progression of distinct stages of rat placental development. TFAP2C is a driver of early events in trophoblast cell development and

285 reappears later in gestation as an essential regulator of the invasive trophoblast cell
286 lineage. A subset of TFAP2C actions on trophoblast cells are dependent on gene
287 dosage.
288

289 **Methods**

290 **Animals and tissue collection**

291 Holtzman Sprague–Dawley rats were acquired from Envigo. Animals were maintained
292 in an environmentally controlled facility (14 h light and 10 h dark cycle) with food and
293 water available ad libitum. Timed pregnancies were established using virgin female rats
294 (8 to 10 weeks of age) mated with adult male rats (>3 months of age). Mating was
295 confirmed by the presence of sperm in the vaginal lavage and was considered gd 0.5.
296 Pseudopregnant female rats were generated by mating with vasectomized male rats.
297 Detection of a seminal plug was considered day 0.5 of pseudopregnancy. Pregnant rats
298 were euthanized on specific days of gestation. Some placentation sites were frozen
299 intact in dry-ice cooled heptane and stored at -80 °C for subsequent histological
300 analyses, whereas others were dissected into uterine-placental interface, junctional
301 zone, and labyrinth zone compartments as previously described (38, 60). Dissected
302 placentation site compartments and fetuses were weighed, frozen in liquid nitrogen, and
303 stored at -80°C for subsequent biochemical analyses. All protocols using rats were
304 approved by the University of Kansas Medical Center Animal Care and Use Committee.
305

306 **Generation of global and conditional *Tfap2c* mutant rat models**

307 A global mutation at the rat *Tfap2c* locus was generated using CRISPR/Cas9 genome
308 editing technology (61). RNA guides targeting Exon 4 of the *Tfap2c* gene (Supplemental
309 Figure 4, Supplemental Table 4) were assembled with *CRISPR* RNA, trans-activating

310 *CRISPR* RNA, and Cas9 nuclease V3 (Integrated DNA Technologies). Conditional
311 *Tfap2c* disruption by the insertion of loxP sites targeted to 5' and 3' introns flanking Exon
312 4 (Figure 3, Supplemental Table 4, and Supplemental Table 5). Electroporation of
313 constructs were performed into one-cell rat embryos using a NEPA21 electroporator
314 (Nepa Gene Co Ltd). Electroporated embryos were transferred to pseudopregnant rats.
315 Offspring were screened for mutations by polymerase chain reaction (**PCR**), and the
316 deletion confirmed by DNA sequencing (GeneWiz). A founder mutant animal was
317 backcrossed with wild type rats to evaluate germline transmission. Genotyping and fetal
318 sex chromosome determination were performed as previously described (47, 61, 62).
319 DNA was extracted from tail-tip biopsies with Red Extract-N-Amp tissue PCR kit (XNAT-
320 1000RXN, Sigma-Aldrich) and used for genotyping. Primers used for genotyping of
321 global and conditional mutations and sex chromosome determinations are provided
322 (Supplemental Table 6). Body weight measurements were performed on offspring
323 generated from specific intercrosses.
324
325 **Reverse transcription-quantitative PCR (RT-qPCR)**
326 Total RNA was isolated from tissues with TRIzol (15596018, Thermo Fisher).
327 Extracted RNA (1 µg) was used to synthesize complementary DNA using a High-
328 Capacity Reverse Transcription kit (4368814, Applied Biosystems) and then diluted 1:10
329 in water. qPCR was performed using PowerSYBR Green PCR Master Mix (4367659,
330 Thermo Fisher) and transcript-specific primer sets (250 nM). Primer sequences are
331 provided (Supplemental Table 7). QuantStudio 5 Real-Time PCR system (Thermo
332 Fisher) cycling conditions were as follows: an initial step (95 °C for 10 min), preceded by
333 40 cycles of two-step PCR (95 °C for 15 s, 60 °C for 1 min), and then a dissociation step
334 (95 °C for 15 s, 60 °C for 1 min), and a sequential increase to (95 °C for 15 s). Relative

335 mRNA expression was calculated using the ΔΔCt method and glyceraldehyde 3-
336 phosphate dehydrogenase was used as a reference RNA.

337 **In situ hybridization**

338 In situ hybridization was performed using the RNAscope® Multiplex Fluorescent
339 Reagent kit version 2 (Advanced Cell Diagnostics) according to the manufacturer's
340 instructions. Images were captured on Nikon 90i upright microscopes (Nikon) with
341 Photometrics CoolSNAP-ES monochrome cameras (Roper). Probes were designed to
342 detect *Tfap2c* (860171, NM_201420.2, target region: 696-1733), *Krt8* (87304-C2,
343 NM_199370.1, target region: 134-1472) and *Prl7b1* (860181-C2, NM_153738.1, target
344 region: 28-900).

345

346 **Immunohistochemistry**

347 Frozen rat placentation sites were sectioned at 10 μm, mounted on slides, and fixed in
348 4% paraformaldehyde. Sections were blocked with 10% goat serum (50062Z, Thermo
349 Fisher) and incubated overnight at 4°C with a primary antibody for vimentin (1:300, sc-
350 6260, Santa Cruz Biotechnology), pan-cytokeratin antibody (1:100, F3418, Sigma-
351 Aldrich), perforin (1:300, TP251, Amsbio), or TFAP2C (1:150, 2320, Cell Signaling
352 Technology). Fluorescence-tagged secondary antibodies, Alexa Fluor 488-conjugated
353 goat anti mouse IgG (A11001, Thermo Fisher), and Alexa Fluor 568-conjugated goat
354 anti-rabbit IgG (A11011, Thermo Fisher) were used to visualize immunostaining.
355 Sections were counterstained with 4,6-diamidino-2-phenylindole (DAPI, 1:50,000,
356 D1306, Invitrogen). Slides were mounted in Fluoromount-G (0100-01, SouthernBiotech)
357 and imaged on Nikon 90i upright microscopes with Photometrics CoolSNAP-ES
358 monochrome cameras (Roper). Regions of the uterine-placental interface possessing

359 cytokeratin-positive cells were quantified using ImageJ software, as previously described
360 by our laboratory (63, 64).
361
362 **Western blotting**
363 Tissue lysates were processed using the radioimmunoprecipitation assay lysis
364 buffer (sc-24948A, Santa Cruz Biotechnology) and protein concentrations determined
365 using the DC Protein Assay Kit (5000112, Bio-Rad). Proteins (80 µg/lane) were
366 separated by sodium dodecyl sulfate polyacrylamide gel electrophoresis. Separated
367 proteins were electrophoretically transferred to polyvinylidene difluoride membranes
368 (10600023, GE Healthcare) for 1 h at 25 V on a semi-dry transfer apparatus (Bio-Rad).
369 Membranes were subsequently blocked with 5% milk for 1 h at room temperature,
370 followed by incubation with antibodies to TFAP2C (1:100, sc-12762, Santa Cruz
371 Biotechnology) in 5% milk overnight at 4°C. After primary antibody incubation, the
372 membranes were washed in Tris-buffered saline with Tween 20 (TBS-T) three times (10
373 min/wash) at room temperature. The membranes were then incubated with anti-mouse
374 immunoglobulin G conjugated to horseradish peroxidase (HRP; 1:5000, Cell Signaling
375 Technology) in 5% milk for 1 h at room temperature, washed in TBS-T three times (10
376 min/wash) at room temperature, immersed in Immobilon Crescendo Western HRP
377 Substrate (WBLUR0500, Sigma-Aldrich), and luminescence detected using Chemi Doc
378 MP Imager (Bio-Rad).
379
380 **Identification of TFAP2C and potential TFAP2C gene targets in rat invasive**
381 **trophoblast cells**
382 Uniform manifold approximation and projection (**UMAP**) plots for *Tfap2c* and *Prl7b1*
383 were generated from rat gd 19.5 uterine-placental interface single cell RNA sequencing

384 (accession No. GSE206086, (38)). Gene expression profiles and open chromatin
385 containing TFAP2C DNA binding motifs identified in rat invasive trophoblast cells (38,
386 41) were integrated and ascribed function through manual annotation using the UniProt
387 (https://www.uniprot.org) and National Center for Biotechnology
388 (https://www.ncbi.nlm.nih.gov/) databases.
389

390 **Statistical analysis**

391 Statistical analyses were performed with GraphPad Prism 10.2.3 software. Statistical
392 comparisons were evaluated using Student's *t* test or one-way ANOVA with Tukey's or
393 Dunnett's post hoc tests as appropriate. Statistical significance was determined as
394 $P<0.05$.
395

396 **Author Contributions**

397 E.M.D., K. I., and M.J.S. conceived and designed the research; E.M.D. and A.M-I.,
398 performed experiments; K.I. provided experimental tools for analysis; E.M.D., A.M-I.,
399 R.L.S, and M.J.S. analyzed the data and interpreted results of experiments; E.M.D. and
400 M.J.S. prepared the manuscript. All authors read, contributed to editing, and approved
401 the final version of manuscript.
402

403 **Acknowledgments**

404 We thank Brandi Miller, Stacy Oxley, and Leslie Tracy for administrative assistance.
405 The work was supported by the Lalor Foundation (E.M.D., A.M.-I.), Kansas Idea Network
406 of Biomedical Research Excellence, P20 GM103418 (E.M.D, A.M.-I.), NIH grants:
407 HD115834 (A.M.-I.), HD104495 (R.L.S.), HD104071 (K.I.), HD020676 (M.J.S.),
408 HD105734 (M.J.S.), HD112559 (M.J.S.), and the Sosland Foundation (M.J.S.).

409 **References**

410 1. Georgiades P, Ferguson-Smith AC, Burton GJ. Comparative developmental anatomy of the
411 murine and human definitive placentae. *Placenta*. 2002;23(1):3–19.

412 2. Maltepe E, Fisher SJ. Placenta: the forgotten organ. *Annu Rev Cell Dev Biol*. 2015;31:523–552.

413 3. Burton GJ, Fowden AL, Thornburg KL. Placental Origins of Chronic Disease. *Physiol Rev*.
414 2016;96(4):1509–1565.

415 4. Enders AC, Welsh AO. Structural interactions of trophoblast and uterus during hemochorial
416 placenta formation. *J Exp Zool*. 1993;266(6):578–587.

417 5. Roberts RM, Green JA, Schulz LC. The evolution of the placenta. *Reproduction*.
418 2016;152(5):R179-189.

419 6. Hertig AT (Arthur T. *Human trophoblast*. Springfield, Ill. : C. C. Thomas; 1968.

420 7. Vićovac L, Aplin JD. Epithelial-mesenchymal transition during trophoblast differentiation. *Acta*
421 *Anat (Basel)*. 1996;156(3):202–216.

422 8. Pijnenborg R, et al. Review article: trophoblast invasion and the establishment of
423 haemochorial placentation in man and laboratory animals. *Placenta*. 1981;2(1):71–91.

424 9. Ain R, Canham LN, Soares MJ. Gestation stage-dependent intrauterine trophoblast cell
425 invasion in the rat and mouse: novel endocrine phenotype and regulation. *Dev Biol*.
426 2003;260(1):176–190.

427 10. Velicky P, Knöfler M, Pollheimer J. Function and control of human invasive trophoblast
428 subtypes: Intrinsic vs. maternal control. *Cell Adh Migr*. 2016;10(1–2):154–162.

429 11. Kaufmann P, Black S, Huppertz B. Endovascular trophoblast invasion: implications for the
430 pathogenesis of intrauterine growth retardation and preeclampsia. *Biol Reprod*. 2003;69(1):1–7.

431 12. Red-Horse K, et al. Trophoblast differentiation during embryo implantation and formation of
432 the maternal-fetal interface. *J Clin Invest*. 2004;114(6):744–754.

433 13. Pijnenborg R, Vercruysse L, Hanssens M. The uterine spiral arteries in human pregnancy:
434 facts and controversies. *Placenta*. 2006;27(9–10):939–958.

435 14. Harris LK. Review: Trophoblast-vascular cell interactions in early pregnancy: how to remodel
436 a vessel. *Placenta*. 2010;31 Suppl:S93-98.

437 15. Whitley GSJ, Cartwright JE. Cellular and molecular regulation of spiral artery remodelling:
438 lessons from the cardiovascular field. *Placenta*. 2010;31(6):465–474.

439 16. Brosens I, Puttemans P, Benagiano G. Placental bed research: I. The placental bed:
440 from spiral arteries remodeling to the great obstetrical syndromes. *Am J Obstet Gynecol*.
441 2019;221(5):437–456.

442 17. Zhang L, et al. Unraveling the mysteries of spiral artery remodeling. *Placenta*. 2023;141:51–
443 56.

444 18. Hilger-Eversheim K, et al. Regulatory roles of AP-2 transcription factors in vertebrate
445 development, apoptosis and cell-cycle control. *Gene*. 2000;260(1–2):1–12.

446 19. Eckert D, et al. The AP-2 family of transcription factors. *Genome Biol*. 2005;6(13):246.

447 20. Kuckenberg P, Kubaczka C, Schorle H. The role of transcription factor Tcfap2c/TFAP2C in
448 trophectoderm development. *Reprod Biomed Online*. 2012;25(1):12–20.

449 21. Hemberger M, Hanna CW, Dean W. Mechanisms of early placental development in mouse
450 and humans. *Nat Rev Genet*. 2020;21(1):27–43.

451 22. Papuchova H, Latos PA. Transcription factor networks in trophoblast development. *Cell Mol*
452 *Life Sci*. 2022;79(6):337.

453 23. Auman HJ, et al. Transcription factor AP-2gamma is essential in the extra-embryonic lineages
454 for early postimplantation development. *Development*. 2002;129(11):2733–2747.

455 24. Werling U, Schorle H. Transcription factor gene AP-2 gamma essential for early murine
456 development. *Mol Cell Biol*. 2002;22(9):3149–3156.

457 25. Kuckenberg P, et al. The transcription factor TCFAP2C/AP-2gamma cooperates with CDX2 to
458 maintain trophectoderm formation. *Mol Cell Biol*. 2010;30(13):3310–3320.

459 26. Cao Z, et al. Transcription factor AP-2γ induces early Cdx2 expression and represses HIPPO
460 signaling to specify the trophectoderm lineage. *Development*. 2015;142(9):1606–1615.

461 27. Benchetrit H, et al. Extensive Nuclear Reprogramming Underlies Lineage Conversion into
462 Functional Trophoblast Stem-like Cells. *Cell Stem Cell*. 2015;17(5):543–556.

463 28. Kubaczka C, et al. Direct Induction of Trophoblast Stem Cells from Murine Fibroblasts. *Cell*
464 *Stem Cell*. 2015;17(5):557–568.

465 29. Shi D, Kellems RE. Transcription Factor AP-2γ Regulates Murine Adenosine Deaminase Gene
466 Expression during Placental Development*. *Journal of Biological Chemistry*.
467 1998;273(42):27331–27338.

468 30. LiCalsi C, et al. AP-2 family members regulate basal and cAMP-induced expression of human
469 chorionic gonadotropin. *Nucleic Acids Res*. 2000;28(4):1036–1043.

470 31. Sapin V, et al. Differential expression of retinoic acid-inducible (Stra) genes during mouse
471 placentation. *Mech Dev*. 2000;92(2):295–299.

472 32. Ben-Zimra M, et al. Uterine and placental expression of steroidogenic genes during rodent
473 pregnancy. *Molecular and Cellular Endocrinology*. 2002;187(1):223–231.

474 33. Peng L, Payne AH. AP-2 gamma and the homeodomain protein distal-less 3 are required for
475 placental-specific expression of the murine 3 beta-hydroxysteroid dehydrogenase VI gene,
476 Hsd3b6. *J Biol Chem*. 2002;277(10):7945–7954.

477 34. Oztürk A, et al. Proteomic identification of AP2 gamma as a rat placental lactogen II
478 trophoblast cell-specific enhancer binding protein. *Endocrinology*. 2006;147(9):4319–4329.

479 35. Ushizawa K, et al. Global gene expression analysis and regulation of the principal genes
480 expressed in bovine placenta in relation to the transcription factor AP-2 family. *Reprod Biol*
481 *Endocrinol*. 2007;5:17.

482 36. Kidder BL, Palmer S. Examination of transcriptional networks reveals an important role for
483 TCFAP2C, SMARCA4, and EOMES in trophoblast stem cell maintenance. *Genome Res*.
484 2010;20(4):458–472.

485 37. Oikawa M, et al. Generation of Tfap2c-T2A-tdTomato knock-in reporter rats via adeno-
486 associated virus-mediated efficient gene targeting. *Molecular Reproduction and Development*.
487 2022;89(3):129–132.

488 38. Scott RL, et al. Conservation at the uterine–placental interface. *Proceedings of the National*
489 *Academy of Sciences*. 2022;119(41):e2210633119.

490 39. Varberg KM, et al. Extravillous trophoblast cell lineage development is associated with active
491 remodeling of the chromatin landscape. *Nat Commun*. 2023;14(1):4826.

492 40. Kim M, et al. The transcriptional regulatory network modulating human trophoblast stem
493 cells to extravillous trophoblast differentiation. *Nat Commun*. 2024;15(1):1285.

494 41. Vu HTH, et al. Core conserved transcriptional regulatory networks define the invasive
495 trophoblast cell lineage. *Development*. 2023;150(15):dev201826.

496 42. Soares MJ, et al. RAT PLACENTATION: AN EXPERIMENTAL MODEL FOR INVESTIGATING THE
497 HEMOCHORIAL MATERNAL-FETAL INTERFACE. *Placenta*. 2012;33(4):233–243.

498 43. Shukla V, Soares MJ. Modeling Trophoblast Cell-Guided Uterine Spiral Artery Transformation
499 in the Rat. *Int J Mol Sci*. 2022;23(6):2947.

500 44. Knipp GT, Audus KL, Soares MJ. Nutrient transport across the placenta. *Advanced Drug*
501 *Delivery Reviews*. 1999;38(1):41–58.

502 45. Soares MJ, et al. Differentiation of trophoblast endocrine cells. *Placenta*. 1996;17(5–6):277–
503 289.

504 46. Wiemers DO, et al. The mouse prolactin gene family locus. *Endocrinology*. 2003;144(1):313–
505 325.

506 47. Iqbal K, et al. Conditionally mutant animal model for investigating the invasive trophoblast
507 cell lineage. *Development*. 2024;151(2):dev202239.

508 48. Chakraborty D, et al. Natural killer cells direct hemochorial placentation by regulating
509 hypoxia-inducible factor dependent trophoblast lineage decisions. *Proc Natl Acad Sci U S A*.
510 2011;108(39):16295–16300.

511 49. Amoroso EC. The evolution of viviparity. *Proc R Soc Med*. 1968;61(11 Pt 2):1188–1200.

512 50. Li L, et al. Lineage regulators TFAP2C and NR5A2 function as bipotency activators in
513 totipotent embryos. *Nat Struct Mol Biol*. 2024;31(6):950–963.

514 51. Zhu M, et al. Developmental clock and mechanism of de novo polarization of the mouse
515 embryo. *Science*. 2020;370(6522):eabd2703.

516 52. Zhu M, et al. Tead4 and Tfap2c generate bipotency and a bistable switch in totipotent
517 embryos to promote robust lineage diversification. *Nat Struct Mol Biol*. 2024;31(6):964–976.

518 53. Gardner RL, Beddington RS. Multi-lineage “stem” cells in the mammalian embryo. *J Cell Sci*
519 *Suppl*. 1988;10:11–27.

520 54. Rossant J. Stem cells from the Mammalian blastocyst. *Stem Cells*. 2001;19(6):477–482.

521 55. Kaiser S, et al. Reduced Gene Dosage of Tfap2c Impairs Trophoblast Lineage Differentiation
522 and Alters Maternal Blood Spaces in the Mouse Placenta1. *Biology of Reproduction*.
523 2015;93(2):31, 1–13.

524 56. Schemmer J, et al. Transcription factor TFAP2C regulates major programs required for
525 murine fetal germ cell maintenance and haploinsufficiency predisposes to teratomas in male
526 mice. *PLoS One*. 2013;8(8):e71113.

527 57. Loureiro-Campos E, et al. Constitutive deficiency of the neurogenic hippocampal modulator
528 AP2γ promotes anxiety-like behavior and cumulative memory deficits in mice from juvenile to
529 adult periods. *Elife*. 2021;10:e70685.

530 58. Sharma N, et al. Tpbpa-Cre-mediated deletion of TFAP2C leads to deregulation of Cdkn1a,
531 Akt1 and the ERK pathway, causing placental growth arrest. *Development*. 2016;143(5):787–
532 798.

533 59. Latos PA, et al. Elf5-centered transcription factor hub controls trophoblast stem cell self-
534 renewal and differentiation through stoichiometry-sensitive shifts in target gene networks.
535 *Genes Dev*. 2015;29(23):2435–2448.

536 60. Ain R, et al. Phenotypic analysis of the rat placenta. *Methods Mol Med*. 2006;121:295–313.

537 61. Iqbal K, et al. Catechol-O-methyltransferase and Pregnancy Outcome: an Appraisal in Rat.
538 *Reprod Sci*. 2021;28(2):462–469.

539 62. Dhakal P, Soares MJ. Single Step PCR-Based Genetic Sex Determination for Rat Tissues and
540 Cells. *Biotechniques*. 2017;62(5):232–233.

541 63. Rosario GX, Konno T, Soares MJ. Maternal hypoxia activates endovascular trophoblast cell
542 invasion. *Dev Biol*. 2008;314(2):362–375.

543 64. Nteeba J, et al. Poorly controlled diabetes mellitus alters placental structure, efficiency, and
544 plasticity. *BMJ Open Diabetes Res Care*. 2020;8(1):e001243.

545

546

547 **Figures**

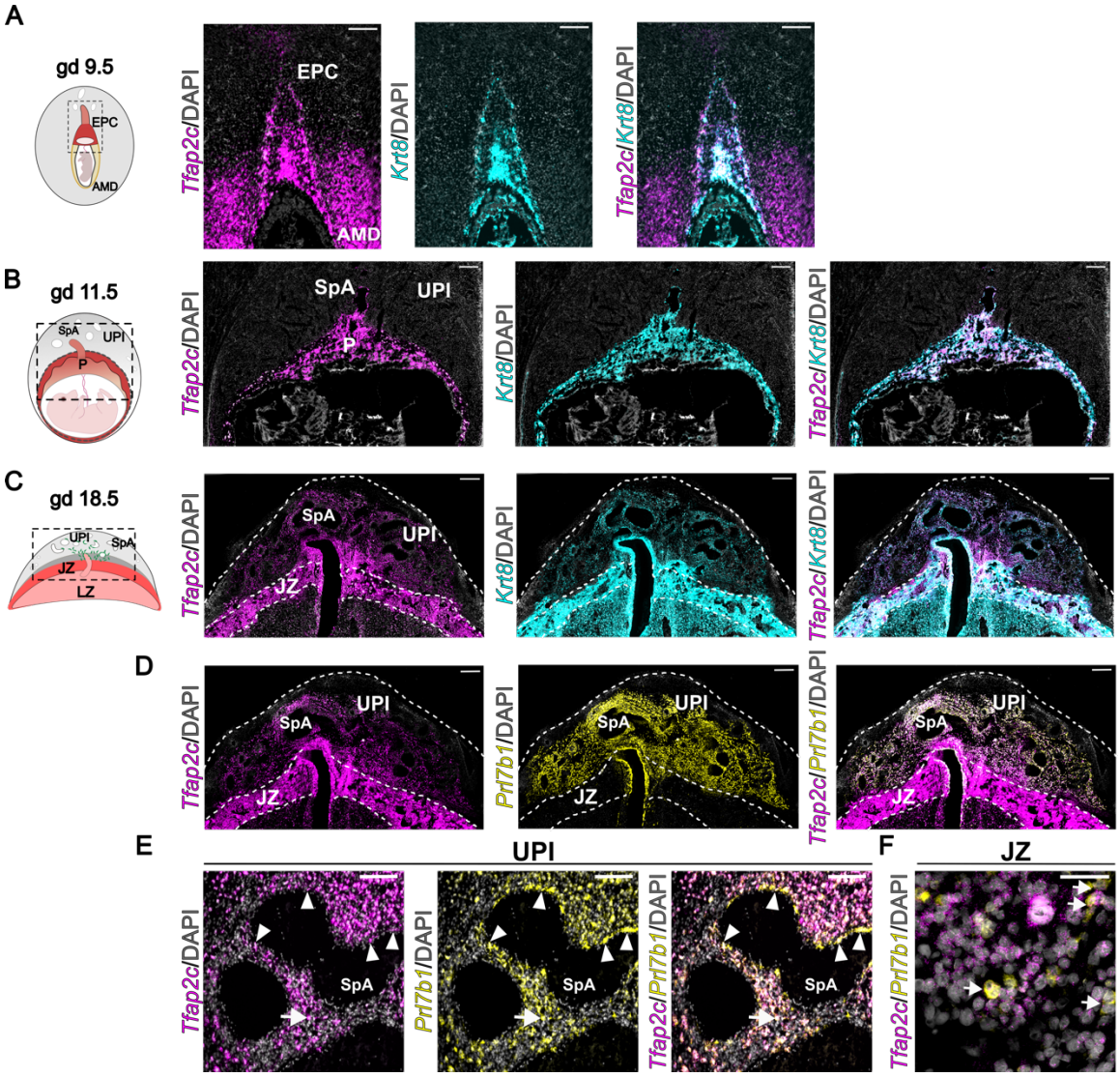

548

549 **Figure 1. *Tfap2c* transcript distribution during placenta development**. **A-C**) *Tfap2c*
550 transcripts (magenta) were localized to the ectoplacental cone at gestation day (gd) 9.5
551 (**A**) and placentation sites at 11.5 (**B**), and 18.5 (**C**). *Tfap2c* transcripts were co-localized
552 with *Krt8* transcripts (cyan). Schematic diagrams representing gd 9.5, 11.5, and 18.5
553 placentation sites are initially presented for each panel. **D**) Co-localization of *Tfap2c*
554 (magenta) and *Prl7b1* (yellow) transcripts within the gd 18.5 placentation site. *Prl7b1* is
555 specifically expressed in the invasive trophoblast cell lineage. Scale bar: 500 μm. **E**)
556 High magnification images showing *Tfap2c* and *Prl7b1* transcript localization in
557 endovascular (arrowhead) and interstitial (arrow) invasive trophoblast cells within the
558 uterine-placental interface. Scale bar: 100 μm. (**F**) Co-localization of *Tfap2c* and *Prl7b1*
559 transcripts (arrows) within the junctional zone of the gd 15.5 placenta. Scale bar: 50 μm.
560 Co-localization is shown as whilte. Abbreviations: EPC, ectoplacental cone; AMD, anti-

561 mesometrial decidua; SpA, spiral artery; UPI, uterine-placental interface; P, placenta; JZ,
562 junctional zone; LZ, labyrinth zone.
563

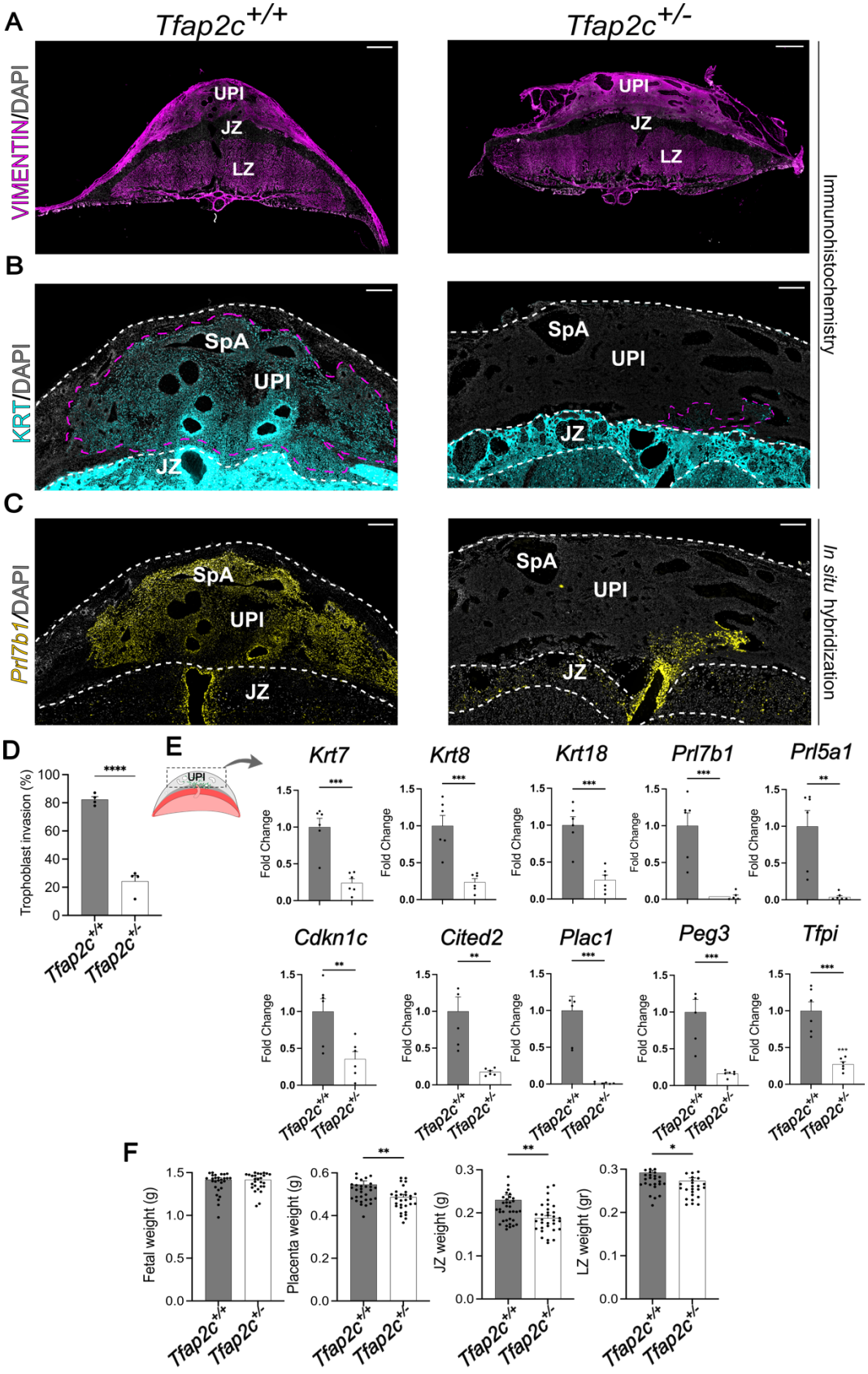
A
Tfap2c+/+
Tfap2c+/-
VIMENTIN/DAPI
UPI
JZ
LZ
Immunohistochemistry
B
KRT/DAPI
SpA
UPI
JZ
C
Prl7b1/DAPI
SpA
UPI
JZ
In situ hybridization
D
Trophoblast invasion (%)
****
Tfap2c+/+
Tfap2c+/-
E
UPI
Krt7
Krt8
Krt18
Prl7b1
Prl5a1
Cdkn1c
Cited2
Plac1
Peg3
Tfpi
Fold Change
F
Fetal weight (g)
Placenta weight (g)
JZ weight (g)
LZ weight (gr)

564

565 **Figure 2. *Tfap2c* gene dosage effects on placental development.** Placentation sites
566 were generated from *Tfap2c*$^{+/-}$ male and *Tfap2c*$^{+/+}$ female breeding. **A)** Identification of
567 placentation site compartments *Tfap2c*$^{+/+}$ and *Tfap2c*$^{+/-}$ using vimentin immunostaining
568 (magenta). **B**) Immunohistochemical localization of cytokeratin protein in gestation day
569 (gd) 18.5 *Tfap2c*$^{+/+}$ and *Tfap2c*$^{+/-}$ placentation sites (cyan). **C**) Distribution of *Prl7b1*
570 transcripts in gd 18.5 *Tfap2c*$^{+/+}$ and *Tfap2c*$^{+/-}$ placentation sites (yellow). **D)** Quantification
571 of trophoblast cell invasion area (magenta dotted line) determined by cytokeratin
572 immunostaining within the uterine-placental interface. Data are expressed as mean ±
573 standard error of the mean (**SEM**). Each data point represents different uterine-placental
574 interface tissues (n=4) obtained from four pregnancies. **E)** RT-qPCR of invasive
575 trophoblast cell-specific transcripts in gd 18.5 *Tfap2c*$^{+/+}$ and *Tfap2c*$^{+/-}$ uterine-placental
576 interface tissues. Data are expressed as mean ± SEM. Each data point represents a
577 biological replicate obtained from six different pregnancies (n=6). **F)** Fetal, placenta,
578 junctional zone and labyrinth zone weights for gd 18.5 *Tfap2c*$^{+/+}$ and *Tfap2c*$^{+/-}$
579 conceptuses. Data are expressed as mean ± SEM. Each data point represents a
580 biological replicate obtained from six different pregnancies (*Tfap2*+$^{+/+}$, n=38; *Tfap2c* $^{+/-}$,
581 n=32). Unpaired *t*-test: * p<0.05, **p<0.01, ***p<0.001, ****p<0.0001. Abbreviations:
582 UPI, uterine-placental interface; JZ, junctional zone; LZ, labyrinth zone; SpA, spiral
583 artery. Scale bars: 500 μm.

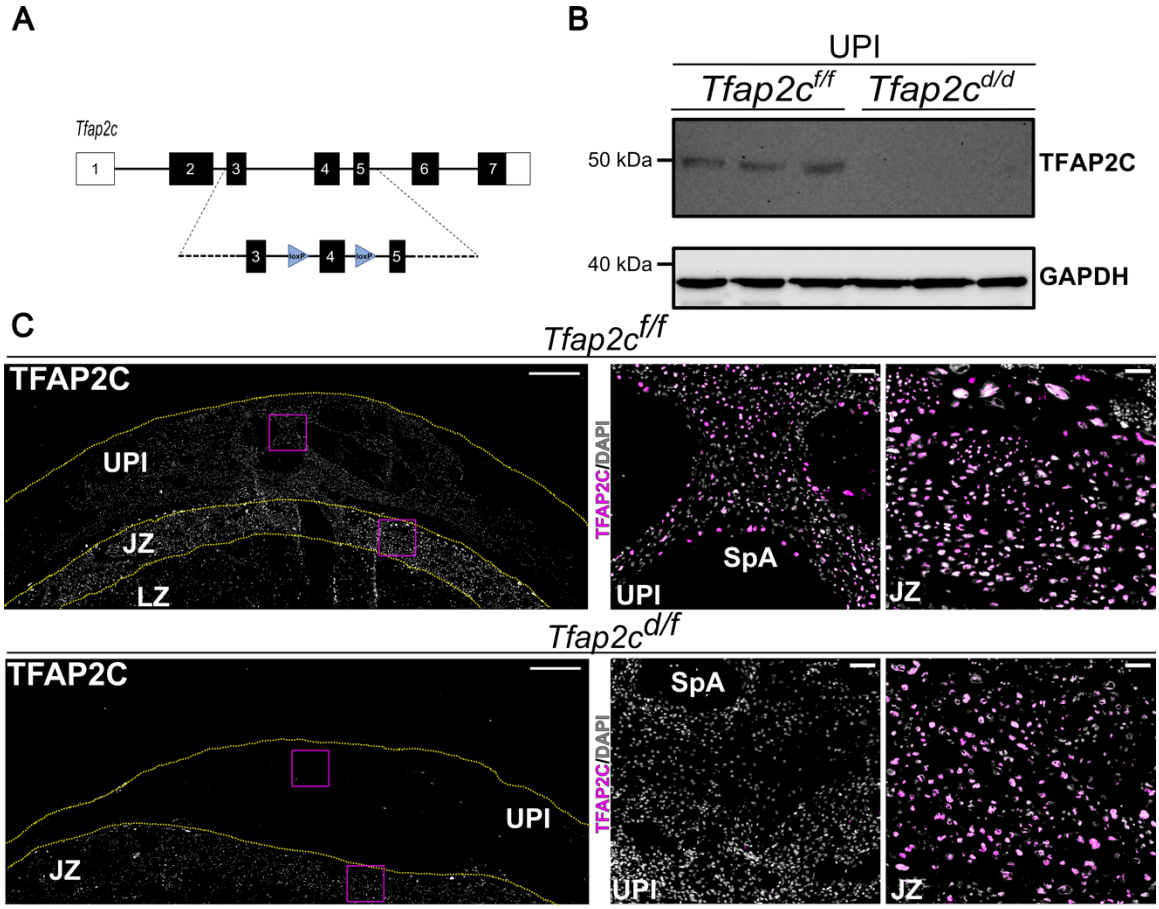

Figure 3. Generation of an invasive trophoblast cell-specific *Tfap2c* deletion. A) Schematic of *loxP* sites inserted into introns flanking Exon 4 of the *Tfap2c* gene. **B)** TFAP2C western blot of the uterine-placental interface of *Tfap2c*$^{f/f}$ and *Tfap2c*$^{d/d}$ gd 18.5 placentation sites. **C)** TFAP2C immunostaining of *Tfap2c*$^{f/f}$ and *Tfap2c*$^{d/d}$ gd 18.5 placentation sites (left panels: TFAP2C immunostaining, white; right panels: TFAP2C immunostaining, magenta, DAPI, white). Scale bar: 500 μm. Inserts to the right show higher magnification images of uterine-placental interface tissues (top) and junctional zone tissue (bottom) for each placentation site. Scale bar: 100 μm. Abbreviations: UPI, uterine-placental interface; JZ, junctional zone; LZ, labyrinth zone; SpA, spiral artery.

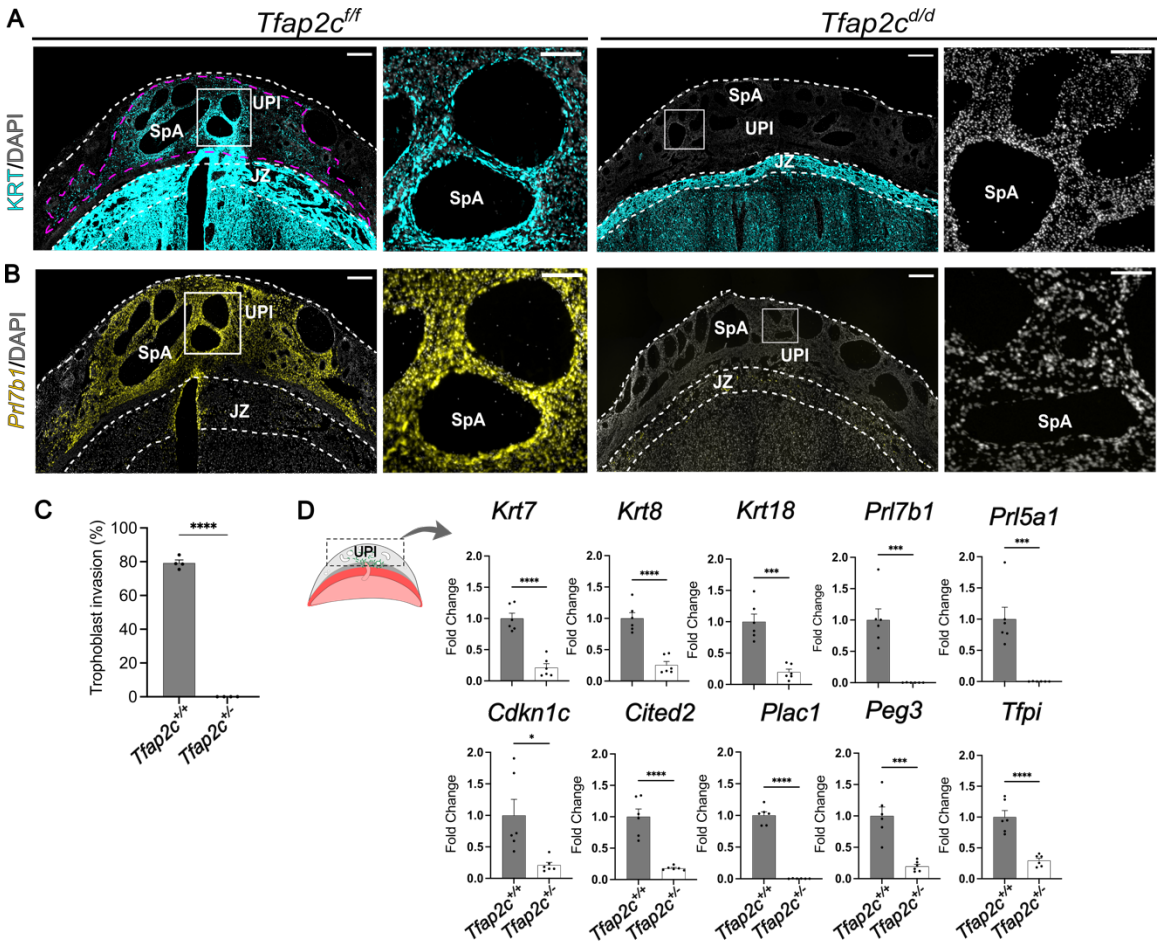

E

Subset of genes expressed in invasive trophoblast cells possessing TFAP2C DNA binding motifs

Extracellular matrix organization	Cell movement - migration	Cytoskeletal organization	Transcriptional regulation
Adamts3, Adgrg6	*Amotl2, Arhagp8,*	*Ankrd17, Apbb1ip*	*Barx2, Bend5*
Col4a1	*Cald1, Dab2ip*	*Cald1, Cfl2*	*Cdx2, Cited2*
Fbln1	*Efnb1, Fbln1*	*Daam1*	*Ets2, Hdac4*
Galnt6	*Mta3, Ncam1*	*Dsp*	*Hic2, Jdp2*
Lama4	*Nuak1, Parva*	*Klhl2*	*Ncor2, Nr2f6*
Lamb1	*Pcdh12, Plet1*	*Krt7*	*Nrip1, Peg3*
Nid1	*Sema6d, Septin4*	*Krt8*	*Pparg, Tfap2c*
Tp53i11	*Svil, Tbc1d9*	*Svil*	*Zfp706*

Figure 4. Characterization of invasive trophoblast cell-specific *Tfap2c* deletion. A) Immunohistochemical localization of cytokeratin (magenta) in gd 18.5 *Tfap2c*$^{f/f}$ and *Tfap2c*$^{d/d}$ placentation sites. **B**) Distribution of *Prl7b1* transcripts (yellow) in gd 18.5 *Tfap2c*$^{f/f}$ and *Tfap2c*$^{d/d}$ placentation sites. Scale bar: 500 μm. Inserts to the right show higher magnification images of the boxed areas within the uterine-placental interface tissues for each placentation site. Scale bar: 100 μm **C)** Quantification of trophoblast cell invasion area (green dotted line) determined by cytokeratin immunostaining within the uterine-placental interface. Data are expressed as mean ± standard error of the mean (**SEM**). Each data point represents different uterine-placental interface tissues obtained from four pregnancies (n=4). **D)** RT-qPCR of invasive trophoblast cell-specific transcripts

606 in gd 18.5 *Tfap2c*$^{f/f}$ and *Tfap2c*$^{d/d}$ uterine-placental interface tissues. The left panel
607 corresponds to a schematic of the regions of the placentation site used for analysis.
608 Data are expressed as mean ± SEM. Each data point represents a biological replicate
609 from six different pregnancies (n=6). **E**) Table of cellular processes potentially regulated
610 by TFAP2C gene targets. Unpaired *t*-test: *p< 0.05, ***p<0.001, ****p<0.0001.).
611 Abbreviations: UPI, uterine-placental interface; JZ, junctional zone; LZ, labyrinth zone;
612 SpA, spiral artery.
613

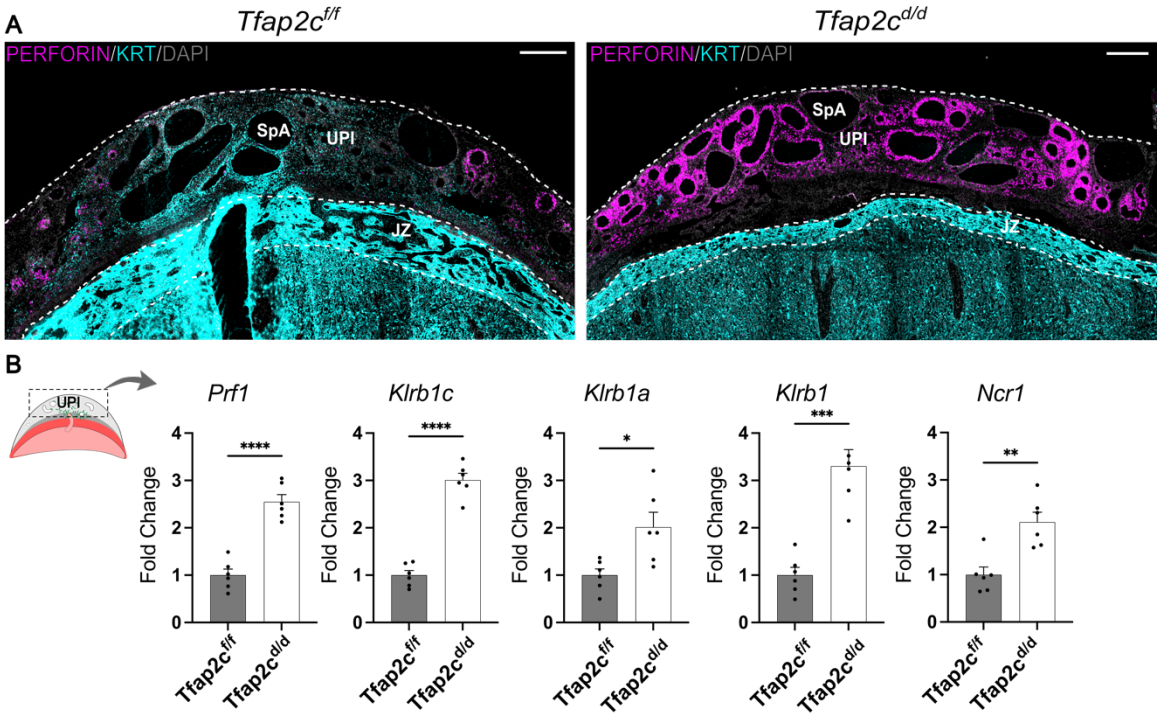

Figure 5. *Tfap2c* conditional deletion in trophoblast invasive cells results in the retention of uterine natural killer (NK) cells within the uterine-placental interface. A) Immunohistochemical localization of cytokeratin (cyan) and perforin (magenta) in gd 18.5 *Tfap2c*$^{f/f}$ and *Tfap2c*$^{d/d}$ placentation sites. **B)** RT-qPCR of NK cell-specific transcripts in gd 18.5 *Tfap2c*$^{f/f}$ and *Tfap2c*$^{d/d}$ uterine-placental interface tissues. The left panel corresponds to a schematic of the regions of the placentation site used for analysis. Data are expressed as mean ± standard error of the mean. Each data point represents a biological replicate from six different pregnancies (n=6). Unpaired *t*-test: *p< 0.05, **p<0.01, ***p<0.001, ****p<0.0001. Abbreviations: UPI, uterine-placental interface; JZ, junctional zone; LZ, labyrinth zone; SpA, spiral artery. Scale bar: 500 μm.

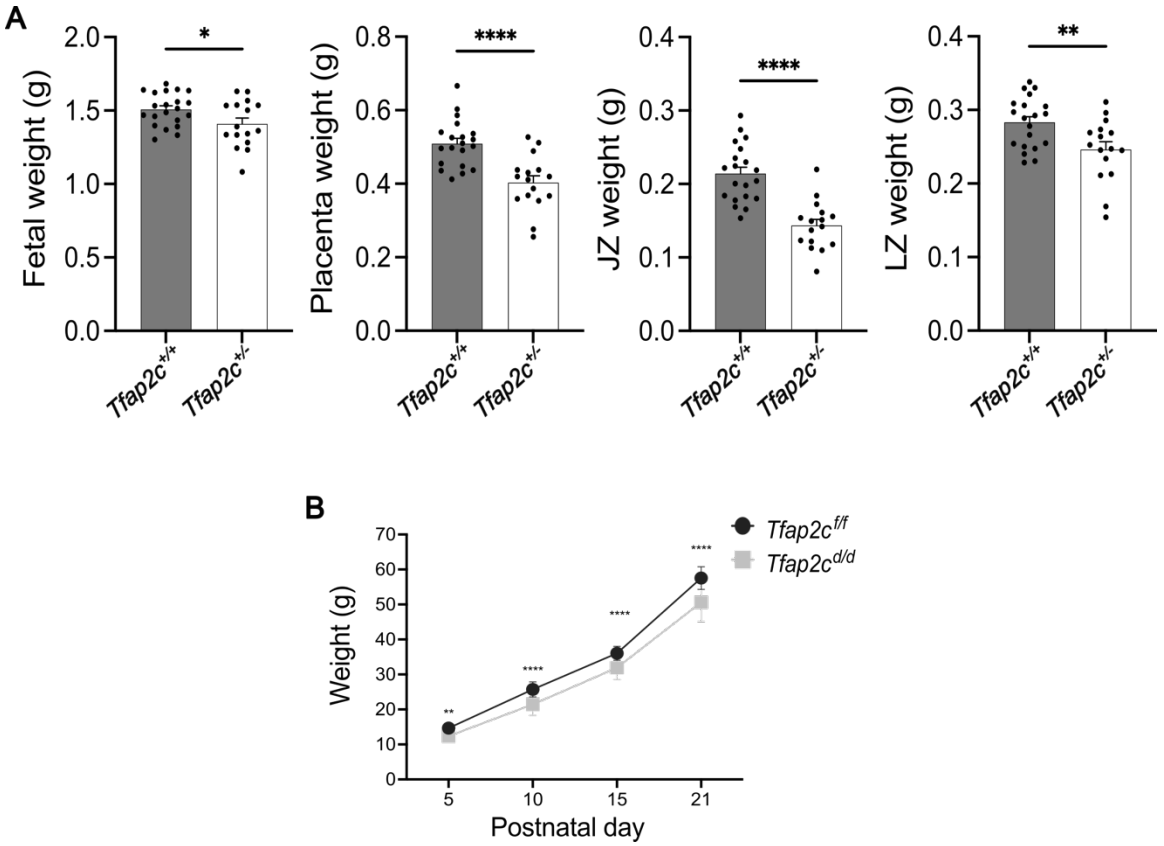

628

629 **Figure 6. Impact of an invasive trophoblast cell-specific *Tfap2c* deletion on**
630 **prenatal and postnatal development. A**) Fetal, placenta, junctional zone, and labyrinth
631 zone weights from gd 18.5 *Tfap2c*$^{f/f}$ and *Tfap2c*$^{d/d}$ gd 18.5 conceptuses. Data are
632 expressed as mean ± standard error of the mean (**SEM**). Each data point represents a
633 biological replicate from six pregnancies (*Tfap2c*$^{f/f}$, n=20; *Tfap2c* $^{d/d}$, n= 16). Unpaired *t*-
634 test: *p< 0.05, **p<0.01, ***p<0.001, ****p<0.0001. **B**) Postnatal body weight for
635 *Tfap2c*$^{f/f}$ and *Tfap2c*$^{d/d}$ pups. Data are expressed as mean ± SEM from six pregnancies
636 (*Tfap2c*$^{f/f}$, n=24; *Tfap2c* $^{d/d}$, n= 29). Two-Way ANOVA and Tukey's Test: **p<0.01,
637 ****p<0.0001. Abbreviations: JZ, junctional zone; LZ, labyrinth zone.
638

639 **Supplemental information**

640 Figures S1 to S6 and Table S1 to S7.

641 Dataset S1. Excel file.